# Functional loss of IκBε leads to NF-κB deregulation in aggressive chronic lymphocytic leukemia

Larry Mansouri,[1] Lesley-Ann Sutton,[1] Viktor Ljungström,[1] Sina Bondza,[1] Linda Arngården,[1] Sujata Bhoi,[1] Jimmy Larsson,[1] Diego Cortese,[1] Antonia Kalushkova,[1] Karla Plevova,[2] Emma Young,[1] Rebeqa Gunnarsson,[1] Elin Falk-Sörqvist,[1] Peter Lönn,[1] Alice F. Muggen,[3] Xiao-Jie Yan,[4] Birgitta Sander,[5] Gunilla Enblad,[1] Karin E. Smedby,[6] Gunnar Juliusson,[7] Chrysoula Belessi,[8] Johan Rung,[1] Nicholas Chiorazzi,[4] Jonathan C. Strefford,[9] Anton W. Langerak,[3] Sarka Pospisilova,[2] Frederic Davi,[10,11] Mats Hellström,[1] Helena Jernberg-Wiklund,[1] Paolo Ghia,[12,13] Ola Söderberg,[1] Kostas Stamatopoulos,[1,14]* Mats Nilsson,[1,15]* and Richard Rosenquist[1]*

[1]Department of Immunology, Genetics, and Pathology, Science for Life Laboratory, Uppsala University, 751 05 Uppsala, Sweden
[2]Central European Institute of Technology, Masaryk University and University Hospital Brno, 601 77 Brno, Czech Republic
[3]Department of Immunology, Erasmus MC, University Medical Center Rotterdam, 3000 CE Rotterdam, Netherlands
[4]The Karches Center for Chronic Lymphocytic Leukemia Research, The Feinstein Institute for Medical Research, Manhasset, NY 11030
[5]Department of Laboratory Medicine, Division of Pathology, Karolinska Institutet and Karolinska University Hospital, 141 86 Huddinge, Stockholm, Sweden
[6]Clinical Epidemiology Unit, Department of Medicine, Karolinska Institutet, 171 76 Stockholm, Sweden
[7]Department of Laboratory Medicine, Lund Stem Cell Center, Lund University, 22184 Lund, Sweden
[8]Hematology Department, General Hospital of Nikea, 18454 Piraeus, Greece
[9]Cancer Sciences Academic Unit, Faculty of Medicine, University of Southampton, Southampton SO16 6YD, England, UK
[10]Department of Hematology, Pitié-Salpêtrière Hospital, F-75013 Paris, France
[11]Cordeliers Research Center, UMR_S 1138, UPMC University of Paris 6, F-75005 Paris, France
[12]Divisione di Oncologia Sperimentale, Dipartimento di Onco-Ematologia, IRCCS Istituto Scientifico San Raffaele and Fondazione Centro San Raffaele, 20132 Milano, Italy
[13]Università Vita-Salute San Raffaele, 20132 Milano, Italy
[14]Institute of Applied Biosciences, Center for Research and Technology Hellas, 57001 Thessaloniki, Greece
[15]Department of Biochemistry and Biophysics, Science for Life Laboratory, Stockholm University, 106 91 Stockholm, Sweden

NF-κB is constitutively activated in chronic lymphocytic leukemia (CLL); however, the implicated molecular mechanisms remain largely unknown. Thus, we performed targeted deep sequencing of 18 core complex genes within the NF-κB pathway in a discovery and validation CLL cohort totaling 315 cases. The most frequently mutated gene was *NFKBIE* (21/315 cases; 7%), which encodes IκBε, a negative regulator of NF-κB in normal B cells. Strikingly, 13 of these cases carried an identical 4-bp frameshift deletion, resulting in a truncated protein. Screening of an additional 377 CLL cases revealed that *NFKBIE* aberrations predominated in poor-prognostic patients and were associated with inferior outcome. Minor subclones and/or clonal evolution were also observed, thus potentially linking this recurrent event to disease progression. Compared with wild-type patients, *NFKBIE*-deleted cases showed reduced IκBε protein levels and decreased p65 inhibition, along with increased phosphorylation and nuclear translocation of p65. Considering the central role of B cell receptor (BcR) signaling in CLL pathobiology, it is notable that IκBε loss was enriched in aggressive cases with distinctive stereotyped BcR, likely contributing to their poor prognosis, and leading to an altered response to BcR inhibitors. Because *NFKBIE* deletions were observed in several other B cell lymphomas, our findings suggest a novel common mechanism of NF-κB deregulation during lymphomagenesis.

CORRESPONDENCE
Richard Rosenquist:
richard.rosenquist@igp.uu.se

Abbreviations used: BcR, B cell receptor; CD40L, CD40 ligand; CLL, chronic lymphocytic leukemia; DLBCL, diffuse large B cell lymphoma; IGHV, Ig heavy variable; IP, immunoprecipitation; TCL, total cell lysate; TTFT, time to first treatment.

*K. Stamatopoulos, M. Nilsson, and R. Rosenquist contributed equally to this paper as senior authors.

Consisting of five members, NFKB1 (p50), NFKB2 (p52), RELA (p65), RELB, and c-REL (REL), the NF-κB signaling pathway regulates many cellular processes, including cell cycle progression, differentiation, and apoptosis (Bonizzi and Karin, 2004). These proteins form homo- and heterodimers that are held in the cytoplasm by inhibitor proteins (IκB) and function by activating or suppressing target genes (Bonizzi and Karin, 2004). The IκBs (α, β, δ, ε, and ζ) are regulated by the IκB kinase complex, which when activated, phosphorylates the IκBs, leading to their degradation; this culminates in the translocation of transcription factors to the nucleus. In B cells, the canonical NF-κB pathway can be activated through numerous upstream signals including B cell receptor (BcR) or TLR signaling, whereas the noncanonical pathway is primarily activated through BAFF receptor–CD40 interaction (Bonizzi and Karin, 2004; Hömig-Hölzel et al., 2008).

Deregulated NF-κB signaling appears to be particularly important in B cell malignancies, with recurrent activating mutations identified in both the canonical and the noncanonical NF-κB pathways (Compagno et al., 2009; Staudt, 2010; Rossi et al., 2013a). In chronic lymphocytic leukemia (CLL), NF-κB activation is known to be present in virtually all cases (Herishanu et al., 2011). That notwithstanding, the extent to which genetic aberrations contribute to NF-κB activation in CLL remains largely unknown except for low-frequency (<3%) mutations in *BIRC3* (noncanonical NF-κB pathway) and *MYD88* (TLR signaling; Baliakas et al., 2015). Very recently, a recurrent 4-bp truncating mutation within the *NFKBIE* gene, which encodes IκBε, a negative regulator of NF-κB in B cells, has been reported as frequent in advanced stage CLL (Damm et al., 2014). However, the precise functional impact of this mutation and, especially, the extent to which it contributes to constitutional NF-κB activation in CLL remain unexplored.

To gain insight into these issues, we undertook a combined genetic and functional approach for investigating the NF-κB signaling pathway in CLL. Taking advantage of HaloPlex technology (Agilent Technologies), we designed a targeted gene panel and performed deep sequencing of 18 members of the NF-κB pathway in 315 CLL cases. The most striking observation was the finding of the recurrent frameshift deletion within the *NFKBIE* gene that resulted in profound functional consequences. In particular, patients carrying this truncating mutation displayed lower IκBε expression and reduced IκBε–p65 interactions, as well as increased levels of phosphorylated p65 and nuclear p50/p65. Because we also detected this truncating event in other lymphoma entities, our finding implies that the loss of IκBε may be a common mechanism contributing to the sustained survival of malignant B cells, thus also shaping disease evolution and ultimately impacting disease progression.

## RESULTS AND DISCUSSION
### Targeted sequencing identifies *NFKBIE* mutations as a recurrent event in CLL

We performed targeted deep sequencing of 18 NF-κB core complex genes (Table S1) within a discovery cohort of 124 CLL patients (Table S2). Sequencing resulted in a mean read depth of 656 reads/base and 97% of the targeted coding regions being covered (Table S1). By applying a conservative cutoff of >10% for the mutant allele, we identified 26 mutations in 11/18 NF-κB genes analyzed within 24/124 (19%) CLL patients (Table S3); 16/16 selected mutations were validated by Sanger sequencing. IκBε (encoded by *NFKBIE*) was the most frequently mutated, being altered in eight patients (6.5%): notably, three/eight patients carried an identical 4-bp frameshift deletion in *NFKBIE* exon 1 (Fig. 1 A). When considering mutations with a low mutant allele frequency (<10%), this 4-bp deletion within *NFKBIE* was found in eight additional cases (Table S4).

*NFKBIE* mutations predominated in CLL cases with unmutated Ig heavy variable (IGHV) genes (U-CLL) belonging to certain subsets with restricted BcR Igs (stereotyped BcRs), for which we and others have reported distinct, subset-biased profiles regarding their biological background and clinical course (Stamatopoulos et al., 2007; Agathangelidis et al., 2012; Strefford et al., 2013; Baliakas et al., 2014). Prompted by this observation, we again performed targeted resequencing of NF-κB genes using HaloPlex technology within a validation CLL cohort (*n* = 191) enriched for cases assigned to poor-prognostic stereotyped subsets (Tables S5 and S6). We found 30 mutations in 10/18 NF-κB genes analyzed within 28 CLL patients; strikingly, 13/30 mutations were in IκBε with 10/13 patients carrying the 4-bp *NFKBIE* deletion (Fig. 1 B and Table S7). This deletion was also detected at a low mutant allele frequency (<10%) in 18 additional cases (Table S4).

Because germline DNA was lacking for the vast majority of patients (because of the retrospective nature of the study), we were limited in our ability to confirm the somatic nature of mutations. That said, we could verify that mutations within the *NFKBIE* gene were somatic and not germline variants in all cases with available material (Tables S3 and S7). For the remaining NF-κB mutations, we cannot formally exclude the possibility that they are rare germline variants (despite extensive filtering against various SNP databases) and hence decided to focus on *NFKBIE*, which, importantly, was also the most frequently mutated NF-κB gene.

### Enrichment of *NFKBIE* aberrations in poor-prognostic subsets of CLL

We next developed a GeneScan assay specific for the 4-bp *NFKBIE* deletion and studied 377 additional CLL cases, including (a) patients from a population-based cohort (Table S8), where U-CLL accounted for 32% of cases, with the remaining cases carrying mutated IGHV genes (M-CLL); (b) patients with stage B/C disease; and (c) patients assigned to stereotyped subsets. Overall, 22 additional *NFKBIE*-deleted patients were identified (Table S9). Collectively, this amounted to 43/692 (6.2%) CLL patients carrying *NFKBIE* aberrations (i.e., mutations and/or deletions), of whom 37/43 concerned U-CLL. A significant enrichment of *NFKBIE* aberrations was observed in certain poor-prognostic stereotyped CLL subsets, especially subset #1 (17/112 cases, 15%) and the less
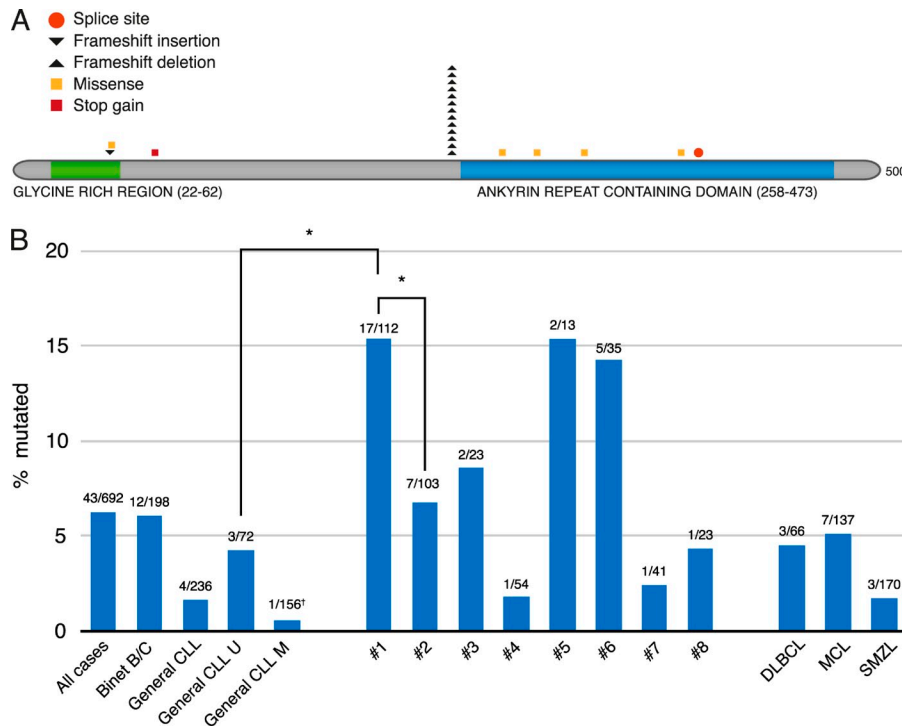
**Figure 1. Recurrent aberrations within the *NFKBIE* gene.** (A) Schematic representation of the human IκBε protein with its key functional domains. Color-coded symbols depict *NFKBIE* alterations with a variant allelic frequency >10% detected in the discovery and validation CLL cohorts using targeted deep sequencing. All missense mutations were predicted to be damaging by the prediction software Polyphen-2. (B) *NFKBIE* mutation frequencies as determined by HaloPlex or GeneScan analysis. The total number of tested cases included in each category is indicated above each bar. Significant differences in *NFKBIE* mutation frequencies between IGHV-unmutated CLL and selected poor-prognostic stereotyped subsets are indicated; a borderline significant trend was also seen when comparing U-CLL with #6 (P = 0.06). * indicates a p-value <0.05. †The only IGHV-mutated case carrying a *NFKBIE* mutation was a poor-prognostic subset #2 patient. CLL U, IGHV-unmutated CLL; CLL M, IGHV-mutated CLL; MCL, mantle cell lymphoma; SMZL, splenic marginal zone lymphoma.

populated subset #6 (5/35 cases, 14%; Fig. 1 B), further supporting the concept that the subclassification of CLL based on BcR stereotypy may supersede the more generic discrimination into U-CLL or M-CLL (Baliakas et al., 2014). A considerably lower frequency of *NFKBIE* aberrations was observed within our population-based cohort (4/236, 1.7%; Smedby et al., 2005), whereas advanced stage B/C patients carried *NFKBIE* aberrations at a frequency of 6.1% (12/198), thus lower than recently reported (10%; Damm et al., 2014).

In Fig. 2 A, we depict coexisting cytogenetic/molecular lesions in the 43 patients with *NFKBIE* aberrations; although a small proportion of cases carried concomitant poor-prognostic *TP53* (7%), *NOTCH1* (14%), and *SF3B1* (9%) mutations, the majority of cases did not carry mutations within these genes. Because mutations have been described in two other NF-κB pathway genes in CLL, *MYD88* and *BIRC3*, albeit at a low frequency (Baliakas et al., 2015), we also sequenced the hotspot p.L265P *MYD88* mutation and exons 6–9 of *BIRC3*. In total, 4/495 (0.8%) patients carried a p.L265P *MYD88* mutation, none of which co-occurred with a mutation in *NFKBIE*, whereas 8/568 (1.4%) patients harbored mutations within *BIRC3*, with only 1 of these patients carrying the 4-bp deletion within *NFKBIE*. In addition, we analyzed copy number data for 369 CLL cases obtained from SNP arrays (250K) and found only 3 cases showing a potential monoallelic deletion covering the *NFKBIE* gene (on chromosome 6p21.1); none of these cases had a truncating *NFKBIE* mutation (not depicted).

The remarkable enrichment of *NFKBIE* aberrations in poor-prognostic subset #1 (17/43 *NFKBIE*-mutated/deleted cases, 39.5%) recalls the significantly higher frequency of *SF3B1*

mutations in poor-prognostic stereotyped subset #2 compared with all remaining CLL (~44% vs. ~5%; Rossi et al., 2013b; Strefford et al., 2013). This subset-biased distribution of genomic aberrations in different poor-prognostic stereotyped subsets supports the existence of distinct mechanisms underlying clinical aggressiveness in CLL and could perhaps result from particular modes of BcR-mediated signaling, which could shape the evolution of each individual subset. In other words, the enrichment seen in stereotyped subsets might primarily be linked to the particular BcR configuration of each subset rather than merely attributed to IGHV gene mutational status.

### *NFKBIE* aberrations are linked to rapid disease progression and poor outcome

The presence of *NFKBIE* aberrations was associated with a significantly shorter time to first treatment (TTFT) similar to IGHV-unmutated or 17p-deleted patients (Fig. 2 B), which was perhaps expected given the preference toward clinically aggressive CLL subsets (Stamatopoulos et al., 2007; Baliakas et al., 2014). In multivariate analysis including established risk factors, *NFKBIE* aberrations did not hold as an independent factor; however, when IGHV mutational status (one of the strongest molecular predictors of TTFT in CLL [Baliakas et al., 2015]) was removed from the model, *NFKBIE* aberrations regained significance (Table S10). Taking into account that almost all cases with *NFKBIE* aberrations concerned U-CLL, this could be the overarching reason behind this latter finding, along with the comparatively lower number of cases in the *NFKBIE*-mutated/deleted group (relative to IGHV-unmutated CLL). Despite a limited number of cases showing
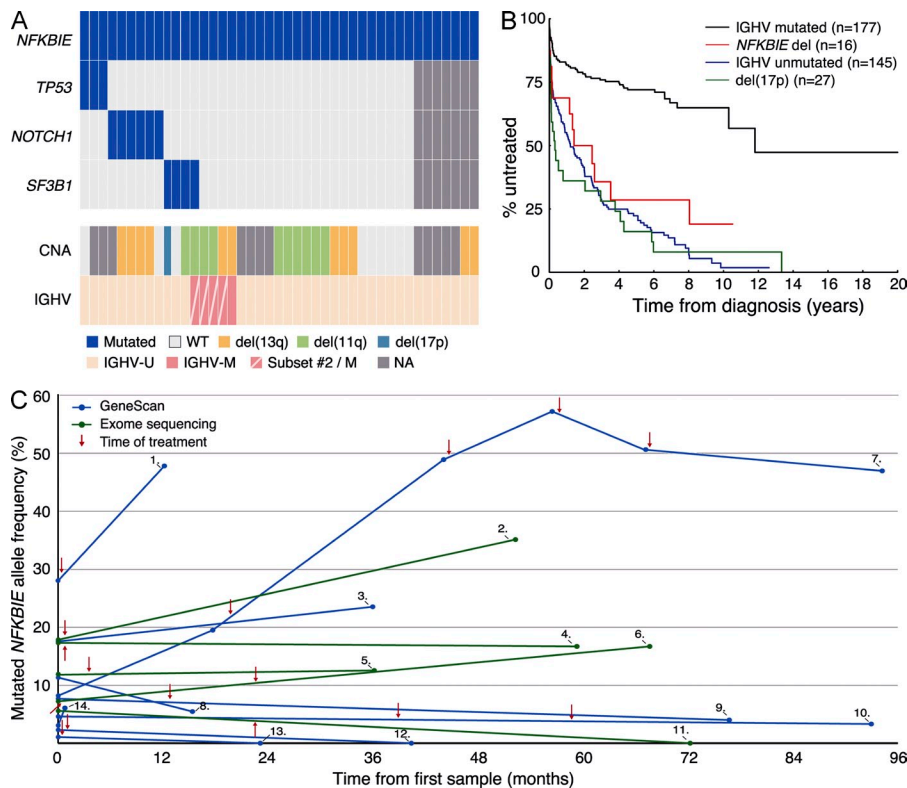
**Figure 2. *NFKBIE* aberrations and associations with clinicobiological data.** (A) Coexisting cytogenetic/molecular aberrations in 43 *NFKBIE*-mutated/deleted cases. (B) TTFT in patients carrying *NFKBIE* aberrations, IGHV-unmutated/mutated genes, or del(17p). (C) Clonal evolution in patients carrying *NFKBIE* aberrations. Dark blue lines indicate samples investigated by GeneScan analysis (nine cases), whereas green lines indicate samples assessed by exome sequencing (five cases). The latter analysis also confirmed the somatic origin of *NFKBIE* aberrations (four deletions and one SNV). Red arrows indicate time of treatment relative to sample collection. In 6/14 cases, clones carrying *NFKBIE* aberrations increased over time. From available mutation data on *TP53*, *SF3B1*, and *NOTCH1*, only two of these cases carried a coexisting *TP53* mutation (case 7 and 14). In case 7, the overall trend and allele frequencies for the mutated *TP53* subclone closely resembled that of the *NFKBIE*-deleted subclone, whereas for case 14, no longitudinal data on *TP53* was available. CNA, copy number aberration; NA, not available.

coexisting *TP53*, *SF3B1*, or *NOTCH1* aberrations, no other clinicobiological factor was identified that could explain the poor outcome seen for the vast majority of cases with *NFKBIE* aberrations, thus implying an important role as a driver mutation during disease evolution.

Because *NFKBIE* aberrations were linked to inferior outcome and considering the finding of low-frequency (<10%) 4-bp *NFKBIE* deletions in a considerable proportion of cases (Table S4), we also investigated longitudinal samples available from 14 treated CLL cases. These cases exhibited varying allele frequencies in the initial sample investigated (8/14 cases <10%, range 1–8%), and an increase in the allelic frequency of the *NFKBIE* mutations and/or deletions was observed over time and at relapse in 6/14 cases (Fig. 2 C). Such temporal dynamics is indicative of clonal evolution and potentially links these aberrations to disease progression. Admittedly, this has to be studied in more detail, in particular because the variant allele frequency of several cases with low-frequency *NFKBIE* aberrations was found to remain stable or essentially unaltered at relapse.

Considering our findings in CLL and the sparse reporting of *NFKBIE* mutations in other lymphomas (Emmerich et al., 2003; Gunawardana et al., 2014), we performed a comprehensive screening of 372 additional mature B cell lymphomas by either targeted sequencing or GeneScan analysis. *NFKBIE* deletions were detected in 7/136 (5.1%) mantle cell lymphomas, 3/66 (4.5%) diffuse large B cell lymphomas (DLBCLs), and 3/170 (1.8%) splenic marginal zone lymphomas. These

results are highly indicative of a common mechanism for NF-κB deregulation within at least a subset of mature B cell malignancy cases (Fig. 1 B).

## IκBε disruption results in reduced inhibition and increased nuclear p65 levels

In normal B cells, IκBε provides negative regulation upon BcR/TLR stimulation by limiting nuclear migration of Rel-containing NF-κB dimers (e.g., p65 and REL) through protein binding via the ankyrin repeat region (Fig. 1 A), thus ensuring temporal control of NF-κB activation (Alves et al., 2014). Furthermore, IκBε loss was reported to result in increased B cell proliferation and survival of stimulated B cells in IκBε$^{-/-}$ mice (Alves et al., 2014). To understand the functional consequence of truncating *NFKBIE* mutations for the NF-κB signaling pathway in CLL, the three IκB members (α, β, and ε) were investigated together with the transcription factor p65 using Western blot analysis. Significantly lower IκBε protein levels were observed in *NFKBIE*-deleted ($n = 7$, mean allele frequency 45%, range 28–61%) versus WT patients ($n = 7$; P < 0.001), whereas no differences were detected for either IκBα or IκBβ (Fig. 3, A–C). Accordingly, phosphorylated p65 levels were significantly higher in *NFKBIE*-deleted versus WT patients (Fig. 3, A–C; P < 0.05).

The 4-bp frameshift *NFKBIE* deletion is predicted to lead to the introduction of a stop codon and subsequent loss of the ankyrin repeat region, thus potentially resulting in a truncated form (with a predicted mass of 13.4 kD) lacking
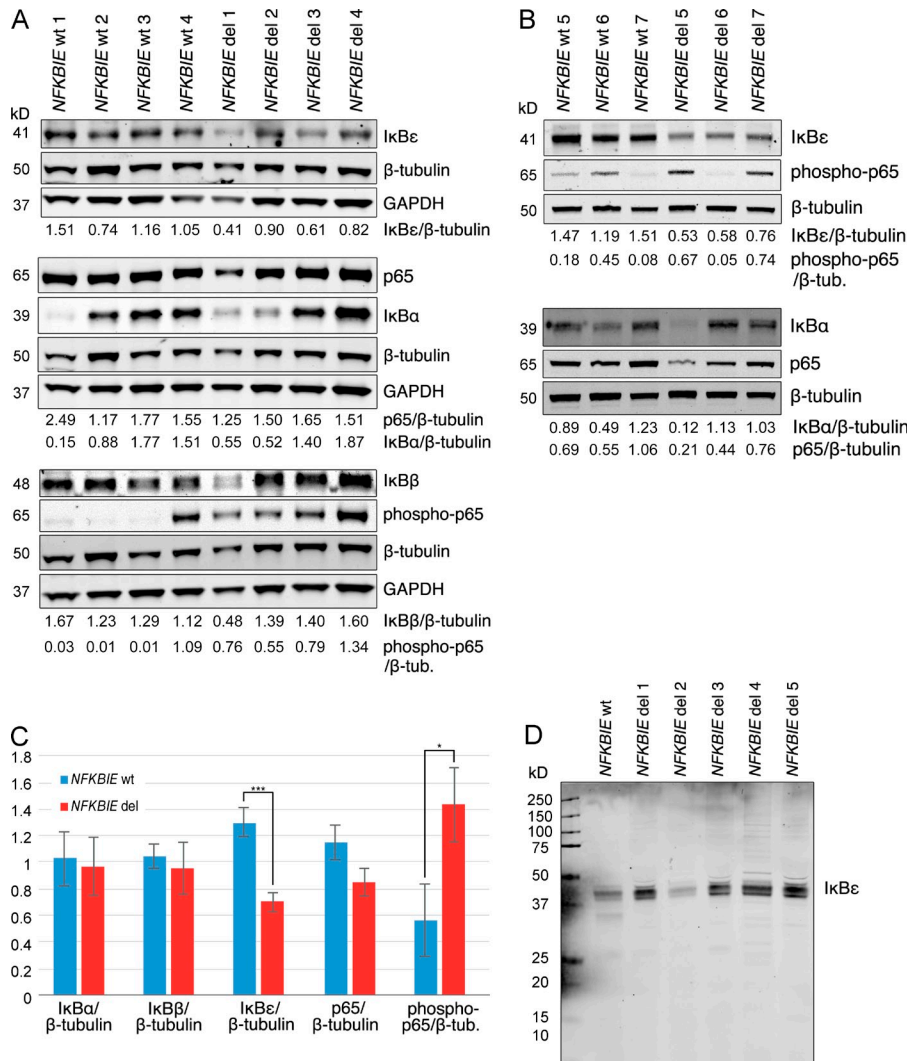
**Figure 3.  Protein expression analysis in NFKBIE–deleted versus WT CLL.** (A) Protein expression profiles of IκBα, IκBβ and IκBε, p65, and phospho-p65 in *NFKBIE*-deleted (n = 4) versus WT (n = 4) CLL by Western blot analysis. (B) Protein expression profiles of IκBα, IκBβ and IκBε, p65, and phospho-p65 in additional *NFKBIE*-deleted (n = 3) versus WT (n = 3) CLL by Western blot analysis. (C) Mean normalized protein expression values for IκBα, IκBβ and IκBε, p65, and phospho-p65 in *NFKBIE*-deleted (n = 7) versus WT CLL (n = 7). * indicates P < 0.05, whereas *** indicates P < 0.001. For IκBβ, only four *NFKBIE*-deleted and four WT CLL cases were assessed. Error bars indicate standard error. (D) Western blot analysis of IκBε in CLL to identify the presence of a truncated IκBε protein. The membrane is overexposed. del, deleted.

this domain, which is a prerequisite for binding to p65 (and other transcription factors). Although both the mutant and WT alleles were expressed at the RNA level in *NFKBIE*-deleted patient samples (Table S11), Western blot analysis for low-molecular mass proteins did not reveal any truncated form of IκBε in *NFKBIE*-deleted cases besides that corresponding to the WT protein (41 kD; Fig. 3 D). Because the truncated form does not appear to render a stable protein, this suggests that the *NFKBIE* deletion may represent a loss-of-function mutation. Regarding the other *NFKBIE* mutations, all of which were missense mutations, these were predominantly located in the ankyrin domain and were deemed as deleterious using various prediction tools (Fig. 1 A).

To further explore how the interaction between IκBε and p65 is influenced, coimmunoprecipitation (co-IP) experiments with p65 demonstrated a lower pull-down of IκBε in *NFKBIE*-deleted (n = 3) versus WT (n = 2) cases (Fig. 4, A and B), indicating reduced interaction between IκBε and p65. Seeking further support for the latter finding, we studied the physical interaction between IκBα, IκBβ and IκBε, and

p65 using an alternative approach by applying proximity ligation assays, a highly sensitive method for real-time visualization of protein–protein interactions in situ (Söderberg et al., 2006). In six *NFKBIE* WT CLL cases, although interactions were detected for all IκBs in unstimulated CLL cells, IκBε exhibited the greatest number of interactions with p65 per cell analyzed, supporting its important role in CLL (Fig. 4 C). Upon stimulation with αIgM or CD40 ligand (CD40L), although the interactions between all IκBs and p65 were reduced, IκBε was predominantly affected (Fig. 4, C–F). In contrast, in six *NFKBIE*-deleted cases, IκBε and p65 interactions in unstimulated CLL cells were notably reduced, thus resembling stimulated WT cells (Fig. 4, C–F); however, this finding did not reach statistical significance (P = 0.15), probably because of the low number of cases available for analysis.

Altogether, our data indicates that these truncating mutations reduce IκBε levels, in turn leading to reduced IκBε–p65 interactions, and, consequently, increasing phosphorylated p65, which is potentially underlying a more activated state. This was further supported by subsequent fractionation experiments
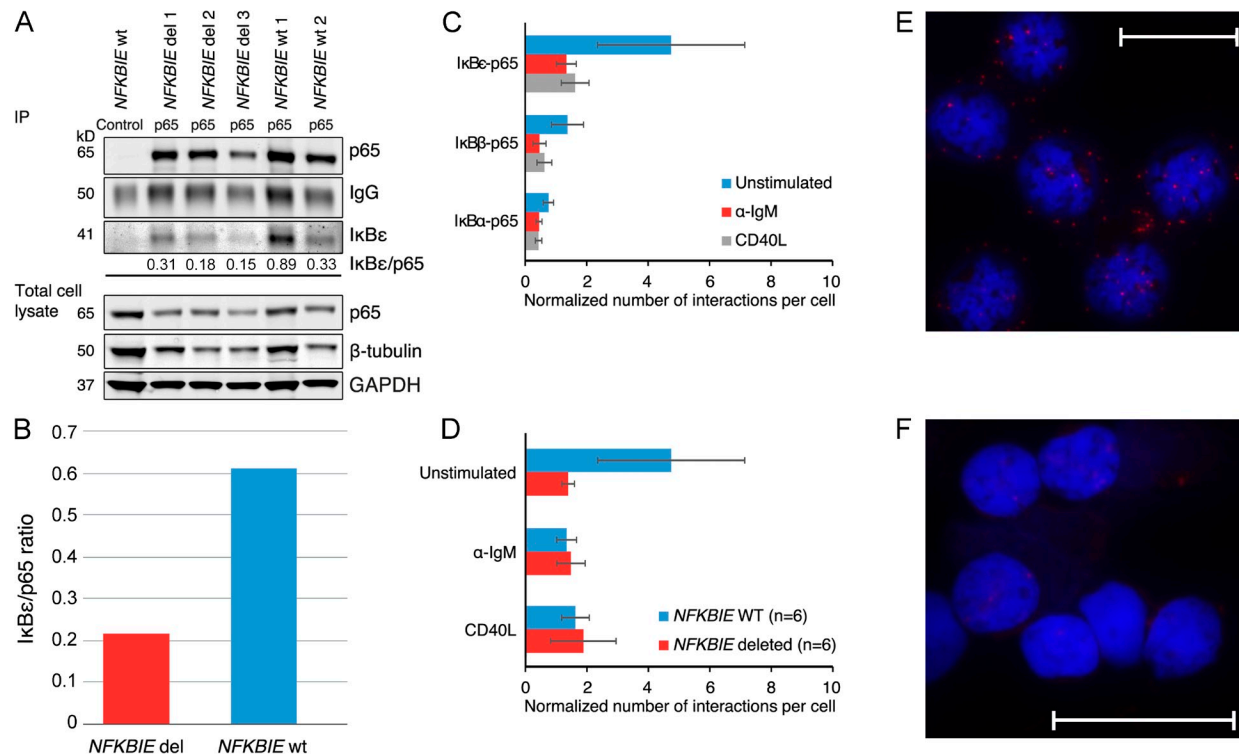
**Figure 4.   Interactions between IκBs and p65 in CLL.** (A) Co-IP to study the interaction between p65 and IκBε in *NFKBIE*-deleted (*n* = 3) versus WT (*n* = 2) CLL. The bottom panel indicates TCL from samples used in the co-IP assay. (B) Mean values for IκBε pull-down in *NFKBIE*-deleted versus WT CLL. (C) Proximity ligation assay to study the physical interaction between IκBα, IκBβ and IκBε, and p65 in six *NFKBIE* WT CLL patients. Interactions were assessed in unstimulated (U), αIgM-stimulated, and CD40L-stimulated cells. For IκBα and IκBε, six *NFKBIE* WT CLL patients were analyzed, whereas for IκBβ only four *NFKBIE* WT CLL patients were assessed. (D) The interaction between IκBε and the transcription factor p65 in six *NFKBIE* WT CLL patients and six *NFKBIE*-deleted patients. Interactions were again assessed in unstimulated (U), αIgM-stimulated, and CD40L-stimulated cells. Error bars indicate standard error. (E and F) Fluorescent microscope images of the interaction between IκBε and the transcription factor p65 in cells from a *NFKBIE* WT CLL patient (E) and an *NFKBIE*-deleted CLL patient (F). Blue color indicates cell nuclei, whereas each red dot represents a single interaction. Bars, 20 µm.

for *NFKBIE*-deleted (*n* = 3) and WT (*n* = 2) samples, which revealed an increase in the nuclear fraction of p50 and p65 in *NFKBIE*-deleted patients (Fig. 5, A–D). Hence, loss of IκBε inhibitory function increased nuclear p50/p65 translocation and consequent NF-κB activation.

### *NFKBIE* deletion has limited impact on the global gene expression profile

To further investigate the impact of this truncating mutation, using shRNA, we knocked down the expression of IκBε (by 56% and 60%, in two independent experiments) in the HG3 CLL cell line (Rosén et al., 2012), which revealed differential gene expression profiles between the knockdowns and the parental as well as the mock-transfected cell line (Fig. 5, E and F; and Table S12). Gene annotation enrichment analysis using the DAVID Bioinformatics Resources revealed that the top annotation clusters included regulation of apoptosis and cell death and regulation of the NF-κB signaling pathway (Table S13). Because the HG3 cell line is EBV transformed, which may seriously interfere with BcR signaling (Siemer et al., 2008), we next studied the global gene expression patterns in primary CLL cells from nine *NFKBIE*-deleted (mean allele frequency

45%, range 28–61%) and nine WT patients. Although an interesting up-regulation of several small nuclear RNAs (i.e., *SNORD66*, *SNORD114-1*, and *SNORA80-B*), previously linked to cancer (Gao et al., 2015), was observed in the *NFKBIE*-deleted group, only a few genes were significantly differentially expressed between the subgroups (Table S14). This finding might reflect previous gene expression profiling studies in U-CLL and M-CLL, showing only subtle differences in gene expression signatures in these clinically distinct subgroups (Klein et al., 2001; Rosenwald et al., 2001); along this line, one gene known to be up-regulated in U-CLL is *ZAP70*, and this gene also showed a higher expression in *NFKBIE*-deleted patients. In addition, as constitutive NF-κB activation has been observed in most, if not all, CLL patients, this may also override potential relevant yet subtler differences in gene expression between *NFKBIE*-deleted and WT patients.

### Altered response to ibrutinib in *NFKBIE*–deleted cases

Finally, because truncating IκBε mutations appeared to lead to constitutive NF-κB activation independent of BcR signaling, we hypothesized that for *NFKBIE*-deleted patients no difference should be observed in the tumor cell response to
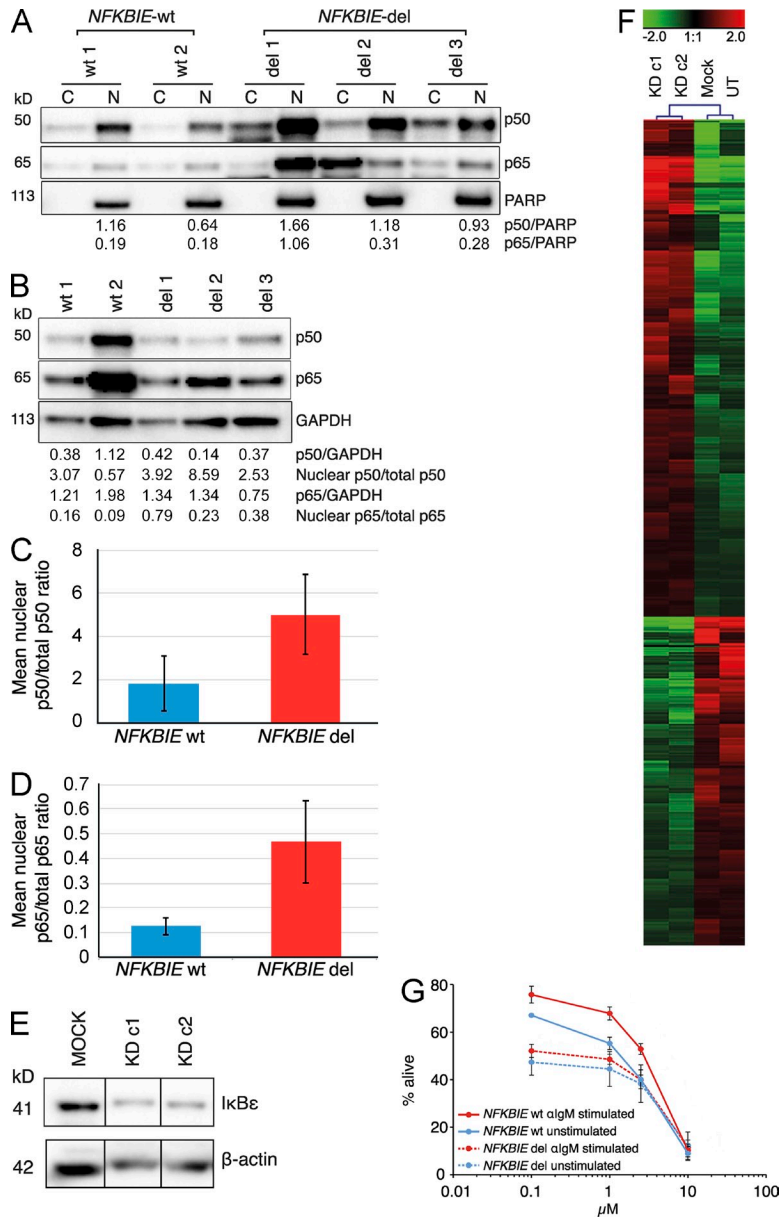
**Figure 5. Functional analysis of the *NFKBIE* deletion in CLL.** (A) Cytoplasmic (C) and nuclear (N) expression of p50, p65, and PARP in CLL patients. For the nuclear fraction, the expression ratio to PARP is provided. (B) Expression levels for p50, p65, and GAPDH in TCLs for the same patient. Normalized nuclear expression for p50 and p65 is provided. (C and D) Mean normalized nuclear expression of p50 (C) and p65 (D) in CLL. Error bars indicate standard error. (E) Western blot showing IκBε expression for the mock-transfected cells as well as the two independent knockdown clones (KD c1 and c2) in the HG3 cell line. All samples were run on the same gel but not in adjacent lanes and have therefore been quantified using the same exposure time. (F) Gene expression patterns in two independent CLL HG3 cell lines (c1 and c2) with partial knockdown (KD) of IκBε compared with the mock-transfected and untransfected (UT) HG3 cell lines. Genes that showed at least 50% difference in both c1 and c2 compared with either Mock or UT were selected. The list of genes is provided in Table S12. (G) Dose–response curves to the BTK inhibitor ibrutinib in primary CLL samples with WT *NFKBIE* (*n* = 4) and deleted *NFKBIE* (*n* = 4). Data were normalized against ibrutinib-naive CLL cells in culture. In *NFKBIE* WT cases, borderline significance was observed when comparing αIgM-stimulated versus unstimulated cells (P = 0.07 at 0.1 μM concentration, P = 0.06 at 1 μM concentration, and P = 0.05 at 2.5 μM concentration). Error bars indicate standard error.

the BcR inhibitor ibrutinib after αIgM stimulation. To test this hypothesis, we treated primary CLL cells from four *NFKBIE*-deleted and four *NFKBIE* WT patients with ibrutinib, in the presence or the absence of αIgM stimulation. A difference in cell survival was observed between unstimulated versus stimulated IκBε-WT cells, whereas no such difference was seen in IκBε-mutated cases (Fig. 5 G), which were generally more sensitive to ibrutinib than WT patients. Although at first sight the finding that *NFKBIE*-deleted cases were generally more sensitive to ibrutinib than WT patients may seem counterintuitive, a similar observation has been reported for the ABC type of DLBCL and has been attributed to tonic activation of the BcR–NF-κB signaling pathway. Thus, along

the same lines, one could reasonably hypothesize that because of tonic BcR signaling, *NFKBIE* mutant CLL cases could be more dependent on external stimulation and, hence, more sensitive to BTK inhibition (Davis et al., 2010; Mathews Griner et al., 2014).

In summary, we provide for the first time a novel genetic basis for NF-κB activation with the prime finding being recurrent mutations in genes belonging to the NF-κB pathway and in particular within the *NFKBIE* gene not only in CLL but also in other B cell–derived malignancies. In CLL, we show that *NFKBIE* aberrations were highly enriched in poor-prognostic, stereotyped subsets, potentially contributing to their adverse prognosis, and resulted in reduced IκBε

protein levels and diminished interactions between IκBε–p65, as well as increased p65 phosphorylation and nuclear translocation. Notably, minor clones and/or clonal evolution were also observed, thus potentially linking IκBε loss to disease progression. Considering the central role of BcR stimulation in the natural history of CLL, the functional loss of IκBε may significantly contribute to sustained CLL cell survival in these patients. On these grounds, components of the NF-κB signaling pathway may emerge as possible targets for future therapies in CLL and, possibly, also other mature B cell lymphomas.

## MATERIALS AND METHODS

**Patient samples.** In total, 692 CLL samples were collected from collaborating institutions in Sweden, Greece, Italy, France, Czech Republic, the Netherlands, the USA, and the UK. All cases were diagnosed according to the iwCLL criteria, displayed a typical CLL immunophenotype, and contained >70% tumor cells (Hallek et al., 2008). Clinicobiological characteristics of the discovery and validation cohorts are summarized in Tables S2 and S5. Mantle cell lymphoma (n = 136), DLBCL (n = 66), and splenic marginal zone lymphoma (n = 170) samples were diagnosed according to the WHO classification. The study was approved by the local Ethics Review Committees (Brno: NT13493-4/2012, Milan: VIVI-CLL, New York: 08-202A, Thessaloniki: CERTH/ETH2, Uppsala: 214/33, Southampton: 06/Q2202/30, and Stockholm: 2006/964-31/2).

**Targeted enrichment and library construction.** We applied HaloPlex technology (Agilent Technologies) for targeted enrichment. For the discovery cohort, an earlier version of the current HaloPlex protocol was used. Biotin-labeled probes were designed for 18 NF-κB genes that targeted all coding exons with a high coverage (Tables S1 and S6). In brief, genomic DNA was fragmented using a combination of restriction enzymes. Biotin-labeled HaloPlex probes were hybridized to the target DNA and acted as template for a second universal DNA oligonucleotide, which contains primer sites, sequencing barcodes, and adapter sequences. The target DNA and the hybridized molecules were captured using streptavidin-labeled magnetic beads and circularized after a ligation reaction. The circularized DNA was amplified using universal primers. For the validation cohort, we took advantage of the automated HaloPlex protocol (http://www.chem.agilent.com/Library/usermanuals/Public/G9900-90020.pdf) using a Bravo Automated Liquid Handling Platform (Agilent Technologies). The libraries were subsequently sequenced using a HiSeq 2000 sequencing system (Illumina).

**Targeted sequencing data analysis.** Illumina adapters were trimmed using Cutadapt, and the reads were aligned to the human genome reference hg19/NCBI GRCh37 using the MOSAIK alignment tool version 2.2 (Martin, 2011). SAMTools was used for file format conversion and sorting. Using a modified version of GATK-lite, the aligned reads were mapped to their corresponding HaloPlex fragment. Variants were detected using an in-house, purpose-built variant caller (SNPmania) and annotated using ANNOVAR (Wang et al., 2010). Exonic variants were kept if they fulfilled the following criteria: (a) having a variant allele ratio of ≥0.1, (b) not in dbSNP and/or 1,000 genomes unless annotated in the Cosmic database, and (c) supported by at least two amplicons unless the position was covered by a single amplicon only.

**Sanger sequencing and GeneScan analysis.** Selected variants were sequenced using the BigDye Terminator v3.1 Cycle Sequencing kit and an ABI 3730 DNA Analyzer (Life Technologies) using standard protocols. For GeneScan analysis, the following oligonucleotides were used for the analysis of the 4-bp deletion in NFKBIE: forward primer, 5′-[Hex]CCTCAAAAGTGGGCTGAG-3′; and reverse primer, 5′-CAAGGAACCACAGGAGAAGG-3′. Genomic DNA was amplified by hot-start PCR with Platinum-Taq DNA Polymerase (Invitrogen) and 60°C as annealing temperature. The fragment length of the PCR products was assessed by capillary electrophoresis with ABI3730XL DNA Analyzer (Applied Biosystems) and analyzed with Peak Scanner Software v1.0 (Applied Biosystems).

**Western blots, co-IP assays, and cell fractions.** Primary CLL cells were washed in PBS and lysed for 10 min in ice-cold RIPA buffer supplemented with phosphatase/protease inhibitors (Roche). Crude cell lysates were cleared by centrifugation and supernatants were transferred to new tubes. For collection of total cell lysates (TCLs), the supernatants were immediately mixed with 4× NuPAGE LDS sample buffer (Life Technologies) with DTT and treated at 95°C for 5 min. For co-IP assays, supernatants were first incubated 2 h at 4°C (end-over-end rotation) with 1:100 addition of either an anti-p65 antibody (a detailed list of all antibodies used is provided in Table S15) or a non-p65–targeting control antibody (AML1) followed by addition of protein A agarose beads (Cell Signaling Technology) and an extra hour of incubation. Beads were collected by centrifugation and washed three times in ice-cold RIPA buffer before being diluted in NuPAGE LDS Sample buffer (Life Technologies) supplemented with DTT and heated at 95°C for 5 min. Nuclear and cytoplasmic cell fractions were obtained as previously described by Andrews and Faller (1991). Denatured samples were separated on NuPAGE Novex 4–12% Bis-Tris Gels (Life Technologies) and transferred to nitrocellulose membranes using iBlot (Life Technologies). Blocking was performed at room temperature by incubating membranes for 1 h in 5% wt/vol nonfat dry milk (Bio-Rad Laboratories) or 5% wt/vol BSA (Sigma-Aldrich) in TBS buffer. Primary antibodies were diluted in TBS-T (0.1% Tween-20) with 5% wt/vol nonfat dry milk (Bio-Rad Laboratories) or 5% wt/vol BSA (Sigma-Aldrich) and were incubated together with the blocked membranes at 4°C over night. Before imaging, membranes were washed (3× 20 min) in TBS-T (0.1% Tween-20), incubated 1 h with secondary antibodies (1:10,000/1:20,000 of the IRDye 800CW goat anti–rabbit IgG and/or 1:20,000 of the IRDye 680RD donkey anti–mouse IgG [LI-COR Biosciences]) in TBS-T (0.1% Tween-20) with 5% wt/vol BSA, washed (3× 15 min) in TBS-T (0.1% Tween-20), and finally rinsed 5 min in TBS buffer only. All incubation steps were performed at room temperature. Membranes were scanned and imaged using the Odyssey CLx Infrared Imaging System (LI-COR Biosciences). Protein bands were quantified using ImageJ software (National Institutes of Health).

**Stimulation of BcR and CD40 signaling pathways.** Two million viable primary CLL cells per milliliter were grown in RPMI medium supplemented with 10% FBS (Gibco), 1% PEST (Gibco), and 1% L-glutamate (Gibco), supplemented with 25% vol/vol serum-free supernatant from the T cell hybridoma cell line MP6 (Rosén et al., 1986), as a source of thioredoxin (Söderberg et al., 1999; Nilsson et al., 2000). For stimulation of the BcR, the modified RPMI medium was supplemented with 3 µg/ml AffiniPure F(ab′)2 fragment rabbit anti–human IgM (Jackson ImmunoResearch Laboratories, Inc.), 10 ng/ml IL-2 (GE Healthcare), and 1 µg/ml streptavidin (Roche). To stimulate the CD40 signaling pathway, cells were treated with the modified RPMI medium supplemented with 100 ng/ml sCD40L (Enzo Life Sciences), 25 ng/ml IL-4 (R&D Systems), and 100 ng/ml IL-10 (R&D Systems). Cells were stimulated for 15 min at 37°C (5% $CO_2$). Cytospins were prepared using 150,000 cells per slide and a Cellspin I cytocentrifuge (Tharmac) at 500 rpm for 2 min.

**Proximity ligation assay.** The cells were fixed in 3.7% formaldehyde solution (Sigma-Aldrich) for 15 min at room temperature and permeabilized in 0.5% Triton X-100 (GE Healthcare) for 2 min at room temperature. All washing steps were performed twice for 5 min in 1× TBS with 0.05% Tween (Sigma-Aldrich) unless stated otherwise. First, the samples were incubated in a blocking solution (Olink Biosciences) for 1 h at 37°C. The primary antibodies were diluted as follows, p65 (Cell Signaling Technology) 1:400, IκBα (Cell Signaling Technology) 1:50, IκBβ (Santa Cruz Biotechnology, Inc.) 1:50, IκBE (Santa Cruz Biotechnology, Inc.) 1:200, and IκBζ (Cell Signaling Technology) 1:50 in antibody diluent solution (Olink Biosciences) and applied to the samples for incubation over night at 4°C. The samples were then washed and incubated with Duolink In Situ PLA Probe

anti–mouse MINUS Affinity donkey anti–mouse IgG and Duolink In Situ PLA Probe anti–rabbit PLUS Affinity donkey anti–rabbit IgG (Olink Bioscience) diluted 1:5 in antibody diluent solution (Olink Biosciences) for 1 h at 37°C, followed by washing. A hybridization solution containing 0.25 mg/ml BSA (New England Biolabs, Inc.), 25 mM NaCl, 0.05% Tween-20 (Sigma-Aldrich), 10 mM TrisAc, 10 mM MgAc, 50 mM KAc, and 125 nM of circularization oligonucleotides (5′-GTTCTGTCATATTTAAGC-GTCTTAA-3′ and 5′-CTATTAGCGTCCAGTGAATGCGAGTCCGT-CTAAGAGAGTAGTACAGCAGCCGTCAAGAGTGTCTA-3′; Integrated DNA Technology) at pH 7.5 were applied to the sample for 30 min incubation at 37°C, followed by washing. Both oligonucleotides were phosphorylated in the 5′ end. Ligation of the circularization oligonucleotides were performed in 1× T4 ligation buffer (Fermentas, Thermo Fisher Scientific), 0.05 U/μl T4 DNA ligase (Fermentas), and ddH$_2$O for 30 min at 37°C, followed by washing. Rolling circle amplification was performed by incubating the samples in 0.25 mg/ml BSA (New England Biolabs, Inc.), 300 ng/ml poly-adenosine, 1× phi29 DNA polymerase buffer (Fermentas), 0.25 mM dNTP (Thermo Fisher Scientific), 1 μM Hoechst 33342 (Sigma-Aldrich), 0.25 U/μl phi29 DNA polymerase (Fermentas), and a BODIPY TR–labeled oligonucleotide (5′-CAGTGAATGCGAGTCCGTCTUUUU-3′, U represents Uracil 2′ O methyl RNA group; Trilink) for 90 min at 37°C. Finally, the samples were washed twice in 1× TBS supplemented with Tween (Sigma-Aldrich) and once in 1× TBS, followed by centrifugation of the slides. SlowFade Gold antifade reagent (Life Technologies) was used for mounting of the slides. Images were acquired with an Axioplan 2 imaging microscope (Carl Zeiss) using 40× objectives and an AxioCam MRm camera (Carl Zeiss). Exposure times, number of z-levels, and distance between z-levels were kept the same for all patients within each assay. CellProfiler version one was used to quantify number of signals per cell in raw images. The interactions between the IκBs and p65 were normalized against the number of interactions between p65 and p50 for each sample.

**Stable knockdown of IκBε.** Stable knockdown of IκBε in the HG3 CLL cell line was established using the pGIPZ lentiviral vector (V3LHS_365665) and the mature antisense sequence 5′-TGGTCCAGATGTACAGCCA-3′ (GE Healthcare). The plasmid was linearized using *Ssp1* restriction enzyme (Fermentas). HG3 cells were transfected with 3 μg of plasmid DNA per 10[7] cells by electroporation using the Neon Transfection System (Thermo Fisher Scientific) and standard parameters. Puromycin selection was started 48 h after transfection and cells were kept under Puromycin selection. Additional selection for positive clones was performed by FACS sorting for cells expressing tGFP, expressed from the same promoter as the shRNA and the Puromycin resistance gene.

**Gene expression analysis.** Gene expression was studied using Affymetrix GeneChip Human Gene 2.0 ST Arrays (Affymetrix) and 250 ng total RNA according to standard protocols. Data were analyzed in R (The R Project for Statistical Computing) using packages from the Bioconductor project and normalized using the robust multi-array average method (Irizarry et al., 2003). To search for differentially expressed genes, an empirical Bayes-moderated Student's *t* test was applied using the "limma" package. The p-values were adjusted using the method of Benjamini and Hochberg to address potential problems with multiple testing (Benjamini and Hochberg, 1995). Genes with an adjusted p-value <0.05 were regarded as differentially expressed. Gene annotation enrichment analysis was performed using the DAVID Bioinformatics Resources.

**Ibrutinib treatment and cell viability test.** Unstimulated and αIgM-stimulated (10 μg/ml for 15 min) primary CLL cells from four *NFKBIE* WT patients and four *NFKBIE*-deleted patients were plated in quadruplicate wells at a density of 100,000 cells per well in 96-well plates followed by ibrutinib (PCI-32765; Selleckchem) treatment at 0, 0.1, 1, 2.5, and 10 μM concentration for 72 h. Alamar Blue (Life Technologies) was added, and cell viability was measured after 24 h using a VICTOR plate reader (PerkinElmer) and standard protocols. Data were normalized against ibrutinib naive matched controls.

**Statistical analysis.** Paired Student's *t* test was used to assess differences between subgroups with at least four patients in each subgroup. Friedman ANOVA was used to study differences in *NFKBIE* mutation frequency among CLL subset cases. Kaplan–Meier analysis was performed to construct survival curves for TTFT, defined as the time interval from the diagnosis date until date of initial treatment, and the log-rank test was used to assess differences. All statistical analyses were performed using Statistica version 12 (Stat Soft).

**Online supplemental material.** Table S1 shows the 18 NF-κB core complex genes targeted for deep sequencing in the discovery cohort. Table S2 shows the clinical and biological characteristics of CLL patients in the discovery cohort. Table S3 shows a summary of mutations found in the discovery cohort ($n = 124$) with additional molecular data. Table S4 shows low-frequency *NFKBIE* deletions (<10%) detected in the discovery ($n = 124$) and validation cohorts ($n = 191$). Table S5 shows clinical and biological characteristics of CLL patients in the validation cohort. Table S6 shows the 18 NF-κB core complex genes targeted for deep sequencing in the validation cohort. Table S7 shows a summary of mutations found in the validation cohort ($n = 191$). Table S8 shows clinical and biological characteristics of the population-based CLL cohort. Table S9 shows a summary of *NFKBIE* deletions detected by GeneScan analysis ($n = 383$). Table S10 shows multivariate analyses for TTFT (A) and for TTFT excluding IGHV mutation status (B). Table S11 shows allelic ratio of the deleted *NFKBIE* allele detected by Gene-Scan analysis. Table S12 shows differentially expressed genes in the HG3 cell line after *NFKBIE* knockdown. Table S13 shows gene annotation enrichment analysis, performed using the DAVID Bioinformatics Resources for differentially expressed genes in HG3 cell line after *NFKBIE* knockdown. Table S14 shows a list of significantly differentially expressed genes in *NFKBIE*-deleted versus *NFKBIE* WT cases. Table S15 shows the list of antibodies used. Online supplemental material is available at http://www.jem.org/cgi/content/full/jem.20142009/DC1.

Author contributions: L. Mansouri, L.-A. Sutton, and V. Ljungström performed research, analyzed data, and wrote the paper. S. Bondza, L. Arngården, S. Bhoi, J. Larsson, D. Cortese, A. Kalushkova, R. Gunnarsson, E. Young, E. Falk-Sörqvist, P. Lönn, K. Plevova, A.F. Muggen, X.-J. Yan, and J. Rung performed research and analyzed data. B. Sander, G. Enblad, K.E. Smedby, G. Juliusson, C. Belessi, N. Chiorazzi, J.C. Strefford, A.W. Langerak, S. Pospisilova, F. Davi, M. Hellström, H. Jernberg-Wiklund, P. Ghia, and O. Söderberg contributed and interpreted data. K. Stamatopoulos, M. Nilsson, and R. Rosenquist designed the study, supervised research, and wrote the paper. All authors contributed to the preparation of the manuscript and approved submission in its current form.

## REFERENCES

Agathangelidis, A., N. Darzentas, A. Hadzidimitriou, X. Brochet, F. Murray, X.J.Yan, Z. Davis, E.J. van Gastel-Mol, C.Tresoldi, C.C. Chu, et al. 2012. Stereotyped B-cell receptors in one-third of chronic lymphocytic leukemia: a molecular classification with implications for targeted therapies. *Blood.* 119:4467–4475. http://dx.doi.org/10.1182/blood-2011-11-393694

Alves, B.N., R.Tsui, J. Almaden, M.N. Shokhirev, J. Davis-Turak, J. Fujimoto, H. Birnbaum, J. Ponomarenko, and A. Hoffmann. 2014. IκBε is a key regulator of B cell expansion by providing negative feedback on cRel and RelA in a stimulus-specific manner. *J. Immunol.* 192:3121–3132. http://dx.doi.org/10.4049/jimmunol.1302351

Andrews, N.C., and D.V. Faller. 1991. A rapid micropreparation technique for extraction of DNA-binding proteins from limiting numbers of mammalian cells. *Nucleic Acids Res.* 19:2499. http://dx.doi.org/10.1093/nar/19.9.2499

Baliakas, P., A. Hadzidimitriou, L.-A. Sutton, E. Minga, A. Agathangelidis, M. Nichelatti, A.Tsanousa, L. Scarfò, Z. Davis, X.-J.Yan, et al. 2014. Clinical effect of stereotyped B-cell receptor immunoglobulins in chronic lymphocytic leukaemia: a retrospective multicentre study. *The Lancet Haematology.* 1:e74–e84. http://dx.doi.org/10.1016/S2352-3026(14)00005-2

Baliakas, P., A. Hadzidimitriou, L.A. Sutton, D. Rossi, E. Minga, N.Villamor, M. Larrayoz, J. Kminkova, A. Agathangelidis, Z. Davis, et al. European Research Initiative on CLL (ERIC). 2015. Recurrent mutations refine prognosis in chronic lymphocytic leukemia. *Leukemia.* 29:329–336. http://dx.doi.org/10.1038/leu.2014.196

Benjamini, Y., and Y. Hochberg. 1995. Controlling the false discovery rate: a practical and powerful approach to multiple testing. *J. R. Stat. Soc., B.* 57:289–300.

Bonizzi, G., and M. Karin. 2004. The two NF-κB activation pathways and their role in innate and adaptive immunity. *Trends Immunol.* 25:280–288. http://dx.doi.org/10.1016/j.it.2004.03.008

Compagno, M., W.K. Lim, A. Grunn, S.V. Nandula, M. Brahmachary, Q. Shen, F. Bertoni, M. Ponzoni, M. Scandurra, A. Califano, et al. 2009. Mutations of multiple genes cause deregulation of NF-κB in diffuse large B-cell lymphoma. *Nature.* 459:717–721. http://dx.doi.org/10.1038/nature07968

Damm, F., E. Mylonas, A. Cosson, K. Yoshida, V. Della Valle, E. Mouly, M. Diop, L. Scourzic, Y. Shiraishi, K. Chiba, et al. 2014. Acquired initiating mutations in early hematopoietic cells of CLL patients. *Cancer Discov.* 4:1088–1101. http://dx.doi.org/10.1158/2159-8290.CD-14-0104

Davis, R.E., V.N. Ngo, G. Lenz, P. Tolar, R.M. Young, P.B. Romesser, H. Kohlhammer, L. Lamy, H. Zhao, Y. Yang, et al. 2010. Chronic active B-cell-receptor signalling in diffuse large B-cell lymphoma. *Nature.* 463:88–92. http://dx.doi.org/10.1038/nature08638

Emmerich, F., S. Theurich, M. Hummel, A. Haeffker, M.S. Vry, K. Döhner, K. Bommert, H. Stein, and B. Dörken. 2003. Inactivating I kappa B epsilon mutations in Hodgkin/Reed–Sternberg cells. *J. Pathol.* 201:413–420. http://dx.doi.org/10.1002/path.1454

Gao, L., J. Ma, K. Mannoor, M.A. Guarnera, A. Shetty, M. Zhan, L. Xing, S.A. Stass, and F. Jiang. 2015. Genome-wide small nucleolar RNA expression analysis of lung cancer by next-generation deep sequencing. *Int. J. Cancer.* 136:E623–E629. http://dx.doi.org/10.1002/ijc.29169

Gunawardana, J., F.C. Chan, A.Telenius, B.Woolcock, R. Kridel, K.L. Tan, S. Ben-Neriah, A. Mottok, R.S. Lim, M. Boyle, et al. 2014. Recurrent somatic mutations of PTPN1 in primary mediastinal B cell lymphoma and Hodgkin lymphoma. *Nat. Genet.* 46:329–335. http://dx.doi.org/10.1038/ng.2900

Hallek, M., B.D. Cheson, D. Catovsky, F. Caligaris-Cappio, G. Dighiero, H. Döhner, P. Hillmen, M.J. Keating, E. Montserrat, K.R. Rai, and T.J. Kipps. International Workshop on Chronic Lymphocytic Leukemia. 2008. Guidelines for the diagnosis and treatment of chronic lymphocytic leukemia: a report from the International Workshop on Chronic Lymphocytic Leukemia updating the National Cancer Institute–Working Group 1996 guidelines. *Blood.* 111:5446–5456. http://dx.doi.org/10.1182/blood-2007-06-093906

Herishanu, Y., P. Pérez-Galán, D. Liu, A. Biancotto, S. Pittaluga, B. Vire, F. Gibellini, N. Njuguna, E. Lee, L. Stennett, et al. 2011. The lymph node microenvironment promotes B-cell receptor signaling, NF-κB activation, and tumor proliferation in chronic lymphocytic leukemia. *Blood.* 117:563–574. http://dx.doi.org/10.1182/blood-2010-05-284984

Hömig-Hölzel, C., C. Hojer, J. Rastelli, S. Casola, L.J. Strobl, W. Müller, L. Quintanilla-Martinez, A. Gewies, J. Ruland, K. Rajewsky, and U. Zimber-Strobl. 2008. Constitutive CD40 signaling in B cells selectively activates the noncanonical NF-κB pathway and promotes lymphomagenesis. *J. Exp. Med.* 205:1317–1329. http://dx.doi.org/10.1084/jem.20080238

Irizarry, R.A., B. Hobbs, F. Collin, Y.D. Beazer-Barclay, K.J. Antonellis, U. Scherf, and T.P. Speed. 2003. Exploration, normalization, and summaries of high density oligonucleotide array probe level data. *Biostatistics.* 4:249–264. http://dx.doi.org/10.1093/biostatistics/4.2.249

Klein, U., Y. Tu, G.A. Stolovitzky, M. Mattioli, G. Cattoretti, H. Husson, A. Freedman, G. Inghirami, L. Cro, L. Baldini, et al. 2001. Gene expression profiling of B cell chronic lymphocytic leukemia reveals a homogeneous phenotype related to memory B cells. *J. Exp. Med.* 194:1625–1638. http://dx.doi.org/10.1084/jem.194.11.1625

Martin, M. 2011. Cutadapt removes adapter sequences from high-throughput sequencing reads. *EMBnet Journal.* 17:10–12. http://dx.doi.org/10.14806/ej.17.1.200

Mathews Griner, L.A., R. Guha, P. Shinn, R.M. Young, J.M. Keller, D. Liu, I.S. Goldlust, A. Yasgar, C. McKnight, M.B. Boxer, et al. 2014. High-throughput combinatorial screening identifies drugs that cooperate with ibrutinib to kill activated B-cell-like diffuse large B-cell lymphoma cells. *Proc. Natl. Acad. Sci. USA.* 111:2349–2354. http://dx.doi.org/10.1073/pnas.1311846111

Nilsson, J., O. Söderberg, K. Nilsson, and A. Rosén. 2000. Thioredoxin prolongs survival of B-type chronic lymphocytic leukemia cells. *Blood.* 95:1420–1426.

Rosén, A., C. Uggla, R. Szigeti, B. Kallin, C. Lindqvist, and J. Zeuthen. 1986. A T-helper cell x Molt4 human hybridoma constitutively producing B-cell stimulatory and inhibitory factors. *Lymphokine Res.* 5:185–204.

Rosén, A., A.C. Bergh, P. Gogok, C. Evaldsson, A.L. Myhrinder, E. Hellqvist, A. Rasul, M. Björkholm, M. Jansson, L. Mansouri, et al. 2012. Lymphoblastoid cell line with B1 cell characteristics established from a chronic lymphocytic leukemia clone by in vitro EBV infection. *OncoImmunology.* 1:18–27. http://dx.doi.org/10.4161/onci.1.1.18400

Rosenwald, A., A.A. Alizadeh, G. Widhopf, R. Simon, R.E. Davis, X. Yu, L. Yang, O.K. Pickeral, L.Z. Rassenti, J. Powell, et al. 2001. Relation of gene expression phenotype to immunoglobulin mutation genotype in B cell chronic lymphocytic leukemia. *J. Exp. Med.* 194:1639–1648. http://dx.doi.org/10.1084/jem.194.11.1639

Rossi, D., C. Ciardullo, and G. Gaidano. 2013a. Genetic aberrations of signaling pathways in lymphomagenesis: revelations from next generation sequencing studies. *Semin. Cancer Biol.* 23:422–430. http://dx.doi.org/10.1016/j.semcancer.2013.04.002

Rossi, D., V. Spina, R. Bomben, S. Rasi, M. Dal-Bo, A. Bruscaggin, F.M. Rossi, S. Monti, M. Degan, C. Ciardullo, et al. 2013b. Association between molecular lesions and specific B-cell receptor subsets in chronic lymphocytic leukemia. *Blood.* 121:4902–4905. http://dx.doi.org/10.1182/blood-2013-02-486209

Siemer, D., J. Kurth, S. Lang, G. Lehnerdt, J. Stanelle, and R. Küppers. 2008. EBV transformation overrides gene expression patterns of B cell differentiation stages. *Mol. Immunol.* 45:3133–3141. http://dx.doi.org/10.1016/j.molimm.2008.03.002

Smedby, K.E., H. Hjalgrim, M. Melbye, A. Torrång, K. Rostgaard, L. Munksgaard, J. Adami, M. Hansen, A. Porwit-MacDonald, B.A. Jensen, et al. 2005. Ultraviolet radiation exposure and risk of malignant lymphomas. *J. Natl. Cancer Inst.* 97:199–209. http://dx.doi.org/10.1093/jnci/dji022

Söderberg, O., U. Thunberg, C. Weigelt, I. Christiansen, T.H. Tötterman, M. Carlsson, J. Sällström, and K. Nilsson. 1999. *Staphylococcus aureus* Cowan strain 1 activation of B-chronic lymphocytic leukaemia cells augments the response to CD40 stimulation. *Scand. J. Immunol.* 50:363–370. http://dx.doi.org/10.1046/j.1365-3083.1999.00604.x

Söderberg, O., M. Gullberg, M. Jarvius, K. Ridderstråle, K.J. Leuchowius, J. Jarvius, K. Wester, P. Hydbring, F. Bahram, L.G. Larsson, and U. Landegren. 2006. Direct observation of individual endogenous protein complexes in situ by proximity ligation. *Nat. Methods.* 3:995–1000. http://dx.doi.org/10.1038/nmeth947

Stamatopoulos, K., C. Belessi, C. Moreno, M. Boudjograh, G. Guida, T. Smilevska, L. Belhoul, S. Stella, N. Stavroyianni, M. Crespo, et al. 2007. Over 20% of patients with chronic lymphocytic leukemia carry stereotyped receptors: Pathogenetic implications and clinical correlations. *Blood*. 109:259–270. http://dx.doi.org/10.1182/blood-2006-03-012948

Staudt, L.M. 2010. Oncogenic activation of NF-κB. *Cold Spring Harb. Perspect. Biol.* 2:a000109. http://dx.doi.org/10.1101/cshperspect.a000109

Strefford, J.C., L.A. Sutton, P. Baliakas, A. Agathangelidis, J. Malčíková, K. Plevova, L. Scarfó, Z. Davis, E. Stalika, D. Cortese, et al. 2013. Distinct patterns of novel gene mutations in poor-prognostic stereotyped subsets of chronic lymphocytic leukemia: the case of SF3B1 and subset #2. *Leukemia*. 27:2196–2199. http://dx.doi.org/10.1038/leu.2013.98

Wang, K., M. Li, and H. Hakonarson. 2010. ANNOVAR: functional annotation of genetic variants from high-throughput sequencing data. *Nucleic Acids Res*. 38:e164. http://dx.doi.org/10.1093/nar/gkq603